Journal of Materials Chemistry C

Accepted Manuscript

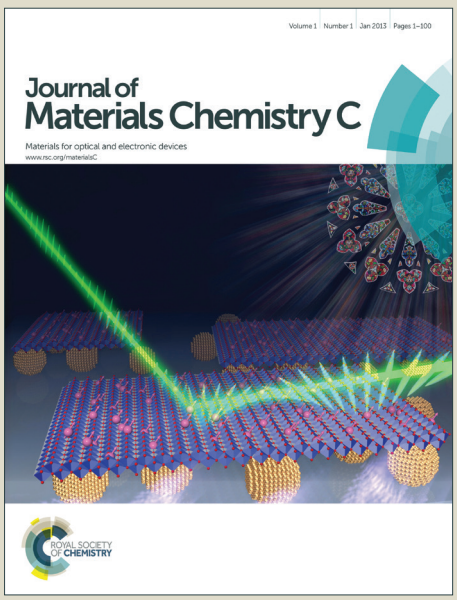

ROYAL SOCIETY OF CHEMISTRY

www.rsc.org/materialsC

Chirality of Self-assembled Metal-Semiconductor Nanostructures

Maozhong Sun[#], Wei Ma[#], Liguang Xu, Libing Wang, Hua Kuang[*], Chuanlai Xu[*]

State Key Lab of Food Science and Technology, School of Food Science and Technology, Jiangnan University, Wuxi, JiangSu, 214122, P. R. China.

ABSTRACT

Plasmonic nanoparticle (NP) chiral dimers have been fabricated using different types of homogenous materials. However, this effect of semiconductor nanoscale dimers is unknown. This paper describes the chiroptical effect of different plasmonic metal-semiconductor hybrid nanostructures composed of gold (Au), silver (Ag) NPs and quantum dots (QDs). Three types of DNA-mediated high yield dimers were obtained, which had a distinct diverse chiroptical effect of peak position and intensity. The semiconductor QDs dimers showed a weak CD signal at 600 nm, while enhanced signals were observed after coupling with Au or Ag NPs. This interesting chiroptical effect, which originated from the assembled chiral geometry, provides a new route for further chiral structures fabrication and applications.

INTRODUCTION

Chiral optical response is an intriguing optical property widely observed in organic and bio-molecules.[1, 2] Although the subtle structural transformation of biomolecules can be detected by observing the circular dichroism (CD) signal in the ultraviolet spectrum range, observation of a chiral molecule with controlled optical response in the visible spectrum range remains challenging.[3, 4] Recently, nanomaterial with excellent optical properties has been used to endow chirality using innovative protocols in the fields of biosensor and applied spectroscopy.[5] Since this new avenue of investigation was opened, based on optical CD in nanoscience,[6-8] vast quantities of interesting research have focused on its origin, transcription, and amplification.[9-11] Significant effort has been directed toward assembling nanoparticles (NPs) into super-structures paralleled with biomolecules, with these particles acting as building blocks for artificial chiral nanostructures.[3, 12] Importantly, a high degree of uniformity in the substrate is essential for observing a non-zero CD signal. To date, a number of sophisticated chiral assemblies utilizing chiral molecules and achiral nanocrystals (NCs) have been reported.[13] Due to the intense interaction between chiral molecules, such as DNA or peptides, and as achiral NCs shape NPs into a chiral form, this may explain the origin of chirality in inorganic materials.[14]

Plasmonic NPs are a rapidly developing nanomaterial in the nanoscale, and their localized surface plasmon resonance (LSPR) arises from resonant oscillations of the conducting electrons with the electromagnetic field around NPs, which can induce plasmonic CD effects.[15, 16] Both theoretical calculations and experiments regarding this property have been reported. [17, 18]

Chiral nanostructures can also be constructed using semiconductor quantum dots (QDs), which have size- and composition-tunable optical properties derived from the quantum confinement effect. Nevertheless, an increasing trend in recent studies is the focus on NCs capped with a chiral ligand, which exhibit different CD signals.[19-23] However, the chiroptical effect in ordered assemblies of QDs is unknown, and thus far, an understanding of the development of chirality is lacking.

Owing to the unique compositions and surface properties of metal and semiconductor materials, it would be interesting to combine them together. Although many studies have focused on their fabrication[24], lattice structure[25], and hybrid properties[26], chirality in these hybrid nanostructures is a new orientation which can

explore the interaction between different materials.

Currently, DNA-based assemblies of NCs show enormous applicability in nanoscience.[27-29] However, the assembly of NPs into well-defined super-structures with stable CD signals is still challenging, and the development of more efficient methods to capitalize on this optical property in the wider field is critically important for the continued advance of this area.[30]

Significant efforts have been made by our group in pursuit of this goal.[31-35] Triggered by different self-organized gold nanorods (NRs), the different twisting directions of two NRs showed enantiomeric conformations and different chiroptical response.[36] Typically, a series of enantiomers was prepared, using different types of pyramids with diverse discrete nanomaterial, and symmetric chiral signals were obtained.[37] Furthermore, to gain insight into this field, we consider that stable chiral performance could also be achieved from dimers based on metal and semiconductor NPs. The simple fabrication method and high homogeneity contribute to efficient chiral platform preparation, and, thus, to strong signal amplification. However, an experimental study of chirality in metal and semiconductor dimers has not previously been demonstrated. In this work, we performed a basic investigation into the intensity and absorption band of the chiroptical signal for different chiral dimer models assembled by Au, Ag and QD NPs. The tailorable chirality which emerged from these assemblies was compared and elaborated comprehensively, which provided solid probative value for further wide-ranging application and research.

EXPERIMENT SECTION

Materials

Hydrogen tetrachloroaurate (III) trihydrate ($HAuCl_4 \cdot 3H_2O$), trisodium citrate, silver nitrate, ascorbic acid (Vc), (1-ethyl-3-(3-Dimethyl aminopropyl) carbodiimide hydrochloride) EDC, (N-hydroxysuccinimide) NHS, poly(vinylpyrrolidone) (PVP) and bis(*p*-sulfonatophenyl)phenylphosphine dihydrate, dipotassium salt (BPS) were purchased from Sigma-Aldrich. CdSe@ZnS core/shell QDs with carboxyl-COOH surface ligands were purchased from Wuhan Jiayuan Quantum Dots Co. Ltd. (Wuhan, China). Thiolated DNA oligonucleotides purified by high performance liquid chromatography (HPLC) were synthesized from Shanghai Sangon Biological

Engineering Technology & Services Co. Ltd. (Shanghai, P.R. China), and dissolved in deionized (DI) water with a final concentration of 100 μM. All glassware was cleaned with freshly prepared aquaregia (HNO_3: HCl=1:3) and rinsed with Millipore-Q water several times. The detailed sequences of the oligonucleotide were:

DNA 1: 5′-CAATAGCCCTTGGATAAAAAAAAAA-SH-3′

DNA 2: 5′-ATCCAAGGGCTATTGAAAAAAAAAA-SH-3′

DNA 3: 5′-CAATAGCCCTTGGATAAAAAAAAAA-NH_2-3′

DNA 4: 5′-ATCCAAGGGCTATTGAAAAAAAAAA-NH_2-3′

Instruments

Ultraviolet-visible (UV-Vis) absorption spectra were collected using UNICO 2100 PC spectrophotometer and processed with Origin Lab software. Transmission electron microscopy (TEM) images were collected with a transmission electron microscope JEOL JEM-2100 operating at an acceleration voltage of 200kV. The size distribution of self-assembly was measured using a Zetasizer Nano ZS system (Malvern) under 633 nm laser. The circular dichroism spectra of nanoassemblies were characterized by MOS-450/AF-Circular Dichroism. Three-dimensional tomographic images were achieved with an FEI Titan Krios equipped with a Gatan UltraScan 4000 (model 895) 16-megapixel CCD under the condition of 300 kV electron accelerating voltage.

DNA Conjugates

The prepared Au and Ag NPs were stabilized in 0.5× TBE buffer containing 50 mM NaCl and coupled with thiolated ssDNA (DNA1, DNA2) in an optimal molar ratio of 1:2 (NPs/DNA) respectively according Scheme. After incubated at room temperature for 12h, uncoupled-DNA was removed though centrifuging and the pellet was redispersed in 0.5× TBE buffer.

QDs were functionalized with amino-modified DNA (DNA3 and DNA4), respectively. Briefly, QDs were diluted with 0.5× TBE and reacted in a molar ratio of 1:1000:200 (QD/EDC/NHS) for 1 h in the dark. Then, DNA was added in a molar ratio of 1:5 (QDs/DNA) and the solution was incubated for 3 h in the dark.

Self-assembly of dimers

For homogenous dimers, NPs functionalized with complementary DNA were mixed in a ratio of 1:1, respectively. For heterodimers, there were some adjustments in the optimal ratio according to calculated molar concentration (Ag-QDs dimer in 1:4, Au-QDs dimer in 1:5). All mixtures were hybridized for 8h with constant shaking in the dark.

Property Characterization

The electrophoresis is performed by 2% agarose gel under the voltage of 100V. 8μL of each samples were loaded in the gel without ethidium bromide.

The circular dichroism spectra of samples were measured under ambient temperature. Samples were added into 1 cm quartz cuvette with a final concentration of 10 nM. The scanning range is from 200 nm to 800 nm.

RESULTS AND DISCUSSION

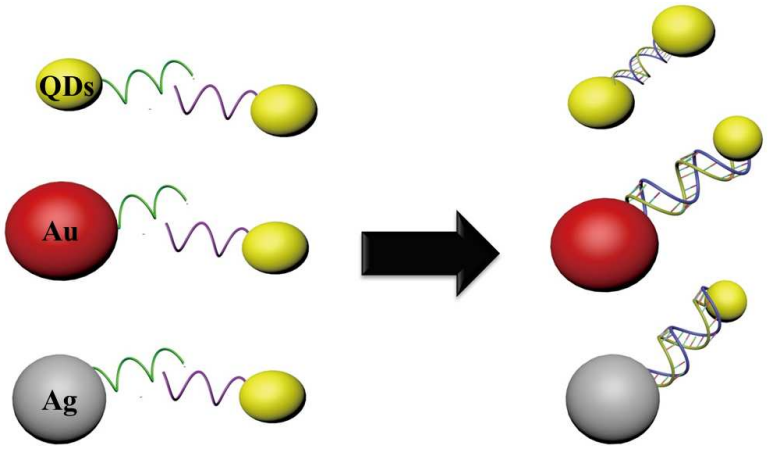

Scheme.1 Schematics of self-assembled chiral dimers

Scheme 1 shows several dimers assembled using various nanomaterials, which reacted under circularly polarized light.

Au NPs with diameters of 10 ± 1.3 nm were synthesized by trisodium citrate reduction of $HAuCl_4$.[38] To obtain stability at high ionic strength, Au NPs were concentrated and modified with the BPS, which will guarantee good dispersion during further processing.[39] Ag NPs with diameters of 10 ± 1.7 nm was prepared following a previously published method with some modifications.[40] The excess layers of PVP surfactant around the particles can prevent spontaneous aggregation. Notably, the stabilizer of BPS and PVP which can avoid non-specific CD signal production are critical for reliable result obtain.

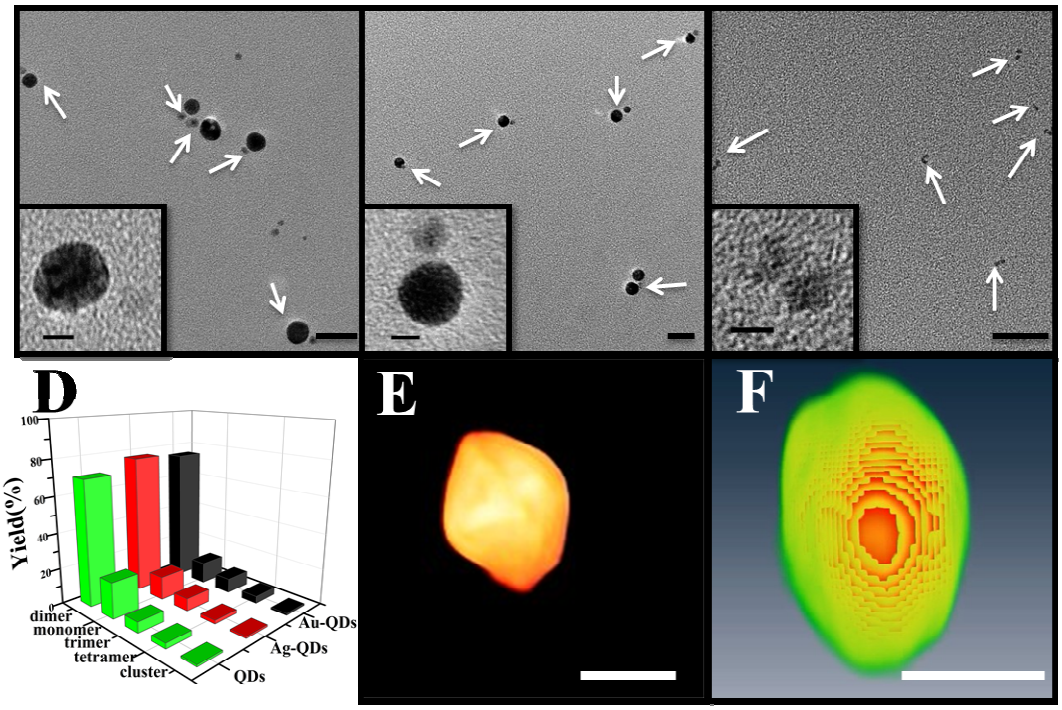

Figure.1 Typical TEM images of the 10nm Au-QDs dimer, scale bar 20nm (A); 10nm Ag-QDs dimer, scale bar 20nm (B); QDs dimer, scale bar 50nm (C); Inset pictures show the magnified assemblies, scale bar 5nm. All dimers were signed with white arrow. Histogram statistics the distribution of various structures after assembly, one hundred NPs were counted randomly for each assembly (D). Typical 3D tomography images of ssDNA-functionalized Au (E) and Ag (F) NP. Scale bar 5nm.

Au and Ag NPs in aqueous solution were functionalized with thiolated DNA oligonucleotides based on a classical method.[41] CdSe@ZnS core/shell QDs with carboxyl-COOH surface ligands were coupled with amino-modified single-stranded DNA (ssDNA), using the EDC and NHS method.[42] The progress of self-assembly was observed by dynamic light scattering (DLS) in aqueous solution (Fig. S1 and Table S1). For all NPs including QDs, Au and Ag NPs, the hydrodynamic diameters were increased from 4.75±0.8nm to 5.97±1.4nm, from 11.3±0.9nm to 11.91±1.3nm and from 10.29±0.7nm to 11.16±1.1nm after surface modification with ssDNA, while the QDs dimer, Au-QDs dimer and Ag-QDs dimer were measured to be 12.72± 1.5 nm, 18.91±1.3 nm and 19.65±1.5 nm, respectively. High yields of the dimers were observed via TEM, and were responsible for significant changes in the CD spectrum (Fig. 1A, B, C and Fig. S3). Furthermore, one hundred assemblies were

counted for statistical distribution of the samples (Fig. 1D). Strikingly, the TEM images show that indeed the particles are not round but often display elongated ellipsoidal shapes. Meanwhile, additional three-dimensional (3D) electron tomography reconstruction images were rendered to further validate this result (Fig. 1E, F). Also, the average aspect ratios of QDs, Au and Ag NPs were statistically calculated to be approximately 1.12±0.2, 1.16±0.4 and 1.21±0.3 according to TEM images, respectively.

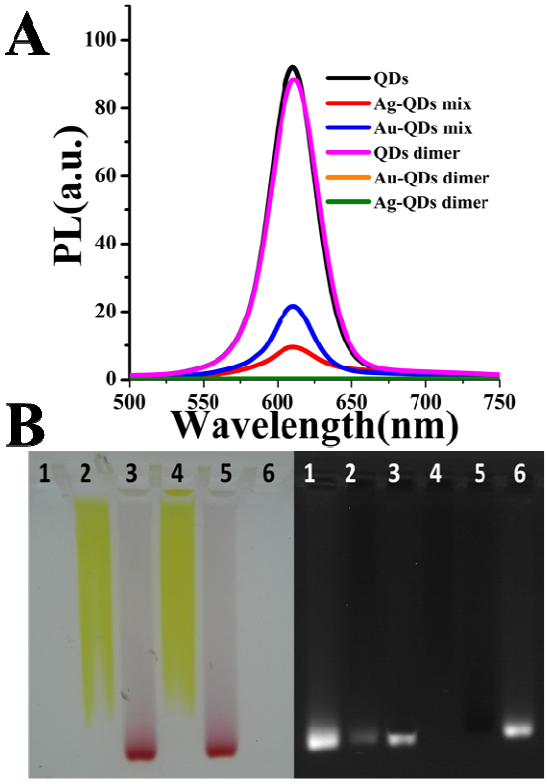

Figure.2 Fluorescent intensity of NPs before and after assembly (A); Agarose gel electrophoretic image of NPs in white (left) and UV light (right) (B). (1) QDs; (2) Ag-QDs mix; (3) Au-QDs mix; (4) Ag-QDs dimer; (5) Au-QDs dimer; (6) QDs dimer.

In control experiments with NPs or NPs mixture bearing non-complementary ssDNA, no dimers were formed. It was important to observe the fluorescent intensity of metal-QDs nanostructures before and after assembly, which was found to change significantly (Fig. 2A). As the high degree formation of Au-QDs and Ag-QDs dimers caused the fluorescence to vanish, this was attributed to the Förster resonance energy transfer (FRET) between adjacent plasmonic metal NPs and QDs.[43] While no obvious

quench, only a slight red shift, was found in QDs dimers, this was due to the electronic coupling and excitation energy transfer in the semiconductor dimers.[44] Furthermore, the fluorescent variation was also proved visually on the electrophoretic image, which also demonstrated the self-assembly process (Fig. 2B).

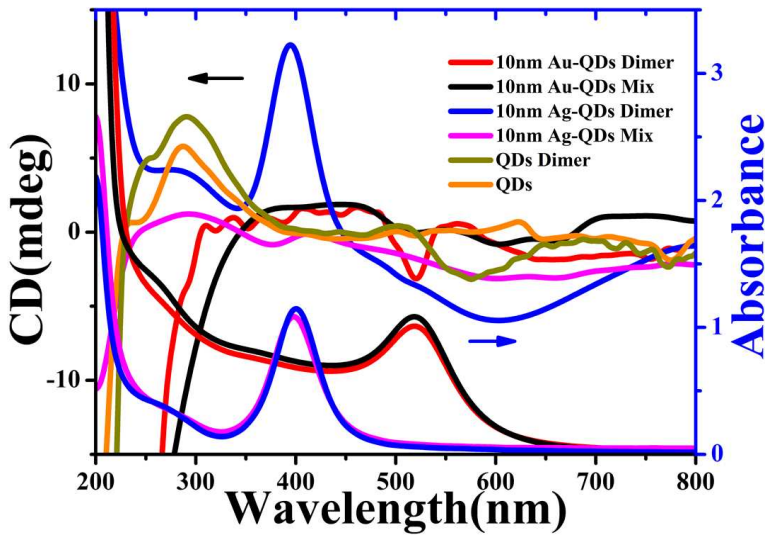

Figure.3 CD and UV-Vis spectrum of 10nm Au-QDs dimer, 10nm Ag-QDs dimer and QDs dimer

Inspired by the extraordinary properties of the metal-semiconductor hybrid nanostructure, we determined the CD effect between plasmonic and semiconductor NPs. As seen in Fig. 3, dimers in different combinations showed unambiguous chiroptical activity as compared with discrete ssDNA functionalized NPs in the corresponding UV-Vis absorption region. This further demonstrated that dimer had a critical role in CD signal generation. Typically, the QDs dimer shows a negative peak of approximately -5 mdeg at 600 nm compared with QDs, which corresponded to their UV-Vis absorption region (Fig. S2B). The Au-QDs heterodimers exhibited a chiral response of approximately -5 mdeg in the Au plasmonic region at 512 nm, while the region of QDs did not exhibit any detectible CD signal. When considering the Ag-QDs heterodimer, a strong positive CD signal about 13 mdeg in the characteristic Ag plasmonic band of 401 nm was obtained, concomitant with a broad, negative response between 500-700 nm, which was stronger than QDs dimers. Evidently, the strength of CD signals in the assemblies intensified, while the absorbance peaks in the UV-Vis spectrum shifted by a small amount. This further illustrated that the CD response was much more sensitive to structural transformation than the UV-Vis spectrum. In terms of these results, the CD intensity not only influenced by the structure of assemblies, but also considerably affected by the neighboring materials.

The chirogenesis of these nanostructures can be explained by the following factors: [32, 35, 45] first, because of the inhomogeneous surface charge distribution of ellipsoidal shaped NPs, DNA preferentially modify on the major axis of NPs due to the low charge density. Under an equilibrium state of the electrostatic repulsion and steric hindrance between adjacent NPs, small angle conformation between two NPs is finally formed. The asymmetrical dipole-dipole interaction between NPs results in the chirality effect in dimers.[46] Thus, the spontaneous orientation of two NPs, linked by DNA, determines the unique enantiomer with preferential angles and chiroptical effect, which can explain the different positive or negative signal in Ag-QDs and Au-QDs dimers. Due to the high electronic oscillation of Ag NPs, the dipole interaction is severe in Ag-QDs dimers. Consequently, it showed a stronger CD response than Au-QDs, which is in accordance with a previous report. On the other hand, a chiral DNA linkage typically displays a bisignated CD line shape in the UV-Vis region (Fig. S2A).[47-49] The chiral molecule dipole could couple with plasmonic NPs via the dynamic Coulomb interaction, so that the chiral response of the dimer structure may be induced from this chiral ligand.[50, 51] However, due to the long distance from the NP surface and only one strand of the double helix was coupled between the NPs, this effect was rather weak.[52] Moreover, the control experiment of ssDNA functionalized NPs with none obvious chiroptical signal could further confirm that the chiral molecules have limited effect for CD signal origin.

CONCLUSIONS

In summary, we have elucidated the chirality in metal-semiconductor and QDs dimer structures. Sufficient efforts have been made to prove that the ellipsoidal shaped NPs can be constructed to a unique enantiomer. This chiral geometry caused by the small twisting angle in these DNA assembled dimers is the primary cause of this effect. Surprisingly, the plasmonic metals especially Ag NPs can give rise to notable enhancement of the CD signal of coupled QDs. Moreover, the self-assembled noble metal-semiconductor dimers open up a new perspective for chiral optical formation, which would have great potential in imaging and sensing.

ACKNOWLEDGEMENTS

This work is financially supported by the National Natural Science Foundation of China (21071066, 91027038, 21101079, 21175034), the Key Programs from MOST (2012BAC01B07, 2012AA06A303, 2012BAD29B04, 2012 BAK11B01, 2011BAK10B07, 2011BAK10B01, 2010AA06Z302, 2010DFB3047, 2013ZX08012-001, 2012BAK17B10, 2012BAK08B01, 2012YQ090194), and grants from Jiangsu Province, MOF and MOE (NCET-12-0879, BE2011626, 201210036, 201310135, 311002, JUSRP51308A).

SUPPORTING INFORMATION

†Electronic Supplementary Information (ESI) available: details of NPs synthesis, DLS images, CD of double-stranded DNA helix, UV-Vis spectrum of QDs NPs and TEM images. See DOI: 10.1039/b000000x/

CORRESPONDING AUTHOR

E-mail: xcl@jiangnan.edu.cn

NOTES AND REFERENCE

1. J. Kypr, I. Kejnovska, D. Renciuk and M. Vorlickova, *Nucleic Acids Res.*, 2009, **37**, 1713-1725.
2. G. Pescitelli, L. Di Bari and N. Berova, *Chem. Soc. Rev.*, 2011, **40**, 4603-4625.
3. A. Kuzyk, R. Schreiber, Z. Fan, G. Pardatscher, E.-M. Roller, A. Högele, F. C. Simmel, A. O. Govorov and T. Liedl, *Nature*, 2012, **483**, 311-314.
4. A. Guerrero-Martinez, J. L. Alonso-Gomez, B. Auguie, M. M. Cid and L. M. Liz-Marzan, *Nano Today*, 2011, **6**, 381-400.
5. Y. Li, Y. Zhou, H. Y. Wang, S. Perrett, Y. Zhao, Z. Tang and G. Nie, *Angew. Chem. Int. Ed. Engl.*, 2011, **50**, 5860-5864.
6. S. Che, Z. Liu, T. Ohsuna, K. Sakamoto, O. Terasaki and T. Tatsumi, *Nature*, 2004, **429**, 281-284.
7. S. Srivastava, A. Santos, K. Critchley, K. S. Kim, P. Podsiadlo, K. Sun, J. Lee, C. L. Xu, G. D. Lilly, S. C. Glotzer and N. A. Kotov, *Science*, 2010, **327**, 1355-1359.
8. S. Srivastava and N. A. Kotov, *Soft Matter.*, 2009, **5**, 1146-1156.
9. Y. Zhao, L. G. Xu, H. Kuang, L. B. Wang and C. L. Xu, *J. Mater. Chem.*, 2012, **22**, 5574-5580.
10. Z. Xu, L. Xu, Y. Zhu, W. Ma, H. Kuang, L. Wang and C. Xu, *Chem. Commun.*, 2012, **48**, 5760-5762.
11. Y. Zhu, L. Xu, W. Ma, Z. Xu, H. Kuang, L. Wang and C. Xu, *Chem. Commun.*, 2012, **48**, 11889-11891.
12. Z. Li, Z. Zhu, W. Liu, Y. Zhou, B. Han, Y. Gao and Z. Tang, *J. Am. Chem. Soc.*, 2012, **134**, 3322-3325.
13. Y. Zhao, L. Xu, L. M. Liz-Marzán, H. Kuang, W. Ma, A. Asenjo-García, F. J. García de Abajo, N. A. Kotov, L. Wang and C. Xu, *J. Phys. Chem. Lett.*, 2013, **4**, 641-647.
14. N. Shukla, M. A. Bartel and A. J. Gellman, *J. Am. Chem. Soc.*, 2010, **132**, 8575-8580.
15. Z. Y. Fan and A. O. Govorov, *Nano Lett.*, 2010, **10**, 2580-2587.

16. M. Chandra, A. M. Dowgiallo and K. L. Knappenberger, *J. Am. Chem. Soc.*, 2012, **134**, 4477-4480.
17. A. O. Govorov, *J. Phys. Chem. C*, 2011, **115**, 7914-7923.
18. A. Guerrero-Martinez, B. Auguie, J. L. Alonso-Gomez, Z. Dzolic, S. Gomez-Grana, M. Zinic, M. M. Cid and L. M. Liz-Marzan, *Angew. Chem. Int. Edit.*, 2011, **50**, 5499-5503.
19. S. D. Elliott, M. P. Moloney and Y. K. Gun'ko, *Nano Lett.*, 2008, **8**, 2452-2457.
20. A. Ben-Moshe, A. O. Govorov and G. Markovich, *Angew. Chem. Int. Edit.*, 2013, **52**, 1275-1279.
21. M. P. Moloney, Y. K. Gun'ko and J. M. Kelly, *Chem. Commun.*, 2007, 3900-3902.
22. T. Nakashima, Y. Kobayashi and T. Kawai, *Angew. Chem. Int. Edit.*, 2009, **131**, 10342-10343.
23. S. A. Gallagher, M. P. Moloney, M. Wojdyla, S. J. Quinn, J. M. Kelly and Y. K. Gun'ko, *J. Mater. Chem.*, 2010, **20**, 8350-8355.
24. A. H. Fu, C. M. Micheel, J. Cha, H. Chang, H. Yang and A. P. Alivisatos, *J. Am. Chem. Soc.*, 2004, **126**, 10832-10833.
25. J. T. Zhang, Y. Tang, K. Lee and O. Y. Min, *Science*, 2010, **327**, 1634-1638.
26. J. M. Luther, P. K. Jain, T. Ewers and A. P. Alivisatos, *Nat. Mater.*, 2011, **10**, 361-366.
27. L. Xu, W. Ma, L. Wang, C. Xu, H. Kuang and N. A. Kotov, *Chem. Soc. Rev.*, 2013, **42**, 3114-3126.
28. L. Xu, H. Kuang, C. Xu, W. Ma, L. Wang and N. A. Kotov, *J. Am. Chem. Soc.*, 2012, **134**, 1699-1709.
29. W. Ma, M. Sun, L. Xu, L. Wang, H. Kuang and C. Xu, *Chem. Commun.*, 2013, **49**, 4989-4991.
30. M. Yang and N. A. Kotov, *J. Mater. Chem.*, 2011, **21**, 6775-6792.
31. W. Yan, W. Ma, H. Kuang, L. Liu, L. Wang, L. Xu and C. Xu, *J. Phys. Chem. C*, 2013, **117**, 17757-17765.
32. L. Xu, C. Hao, H. Yin, L. Liu, W. Ma, L. Wang, H. Kuang and C. Xu, *J. Phys. Chem. Lett.*, 2013, **4**, 2379-2384.
33. Z. Xu, L. Xu, L. M. Liz‐Marzán, W. Ma, N. A. Kotov, L. Wang, H. Kuang and C. Xu, *Adv. Opt. Mater.* 2013, **1**, 626-630.
34. W. Ma, H. Kuang, L. Xu, L. Ding, C. Xu, L. Wang and N. A. Kotov, *Nat. Commun.*, 2013, **4**, 2689.
35. X. Wu, L. Xu, L. Liu, W. Ma, H. Yin, H. Kuang, L. Wang, C. Xu and N. A. Kotov, *J. Am. Chem. Soc.*, 2013, **135**, 18629-18636.
36. W. Ma, H. Kuang, L. B. Wang, L. G. Xu, W. S. Chang, H. N. Zhang, M. Z. Sun, Y. Y. Zhu, Y. Zhao, L. Q. Liu, C. L. Xu, S. Link and N. A. Kotov, *Sci. Rep.*, 2013, **3**.1934.
37. W. J. Yan, L. G. Xu, C. L. Xu, W. Ma, H. Kuang, L. B. Wang and N. A. Kotov, *J. Am. Chem. Soc.*, 2012, **134**, 15114-15121.
38. G. Frens, *Nature*, 1973, **241**, 20-22.
39. S. A. Claridge, S. L. Goh, J. M. J. Frechet, S. C. Williams, C. M. Micheel and A. P. Alivisatos, *Chem. Mater.*, 2005, **17**, 1628-1635.

40. Y. G. Sun and Y. N. Xia, *Adv. Mater.*, 2003, **15**, 695-699.

41. S. J. Hurst, A. K. Lytton-Jean and C. A. Mirkin, *Anal. Chem.*, 2006, **78**, 8313-8318.

42. W. Chen, D. Xu, L. Liu, C. Peng, Y. Zhu, W. Ma, A. Bian, Z. Li, Yuanyuan, Z. Jin, S. Zhu, C. Xu and L. Wang, *Anal. Chem.*, 2009, **81**, 9194-9198.

43. T. Pons, I. L. Medintz, K. E. Sapsford, S. Higashiya, A. F. Grimes, D. S. English and H. Mattoussi, *Nano Lett.*, 2007, **7**, 3157-3164.

44. R. Koole, P. Liljeroth, C. D. Donega, D. Vanmaekelbergh and A. Meijerink, *J. Am. Chem. Soc.*, 2006, **128**, 10436-10441.

45. A. O. Govorov, Z. Y. Fan, P. Hernandez, J. M. Slocik and R. R. Naik, *Nano Lett.*, 2010, **10**, 1374-1382.

46. B. Auguié, J. L. Alonso-Gómez, A. s. Guerrero-Martínez and L. M. Liz-Marzán, *J. Phys. Chem. Lett.*, 2011, 846-851.

47. G. Fukuhara and Y. Inoue, *J. Am. Chem. Soc.*, 2011, **133**, 768-770.

48. M. Caricato, C. Coluccini, D. Dondi, D. A. Vander Griend and D. Pasini, *Org. Biomol. Chem.*, 2010, **8**, 3272-3280.

49. D. P. Iwaniuk and C. Wolf, *J. Am. Chem. Soc.*, 2011, **133**, 2414-2417.

50. H. Zhang and A. O. Govorov, *Phys. Rev. B*, 2013, **87**.

51. A. O. Govorov, Y. K. Gun'ko, J. M. Slocik, V. A. Gerard, Z. Y. Fan and R. R. Naik, *J. Mater. Chem.*, 2011, **21**, 16806-16818.

52. Z. Zhu, J. Guo, W. Liu, Z. Li, B. Han, W. Zhang and Z. Tang, *Angew. Chem. Int. Edit.*, 2013, DOI: 10.1002/ange.201305389.